PHOTONICS Research

Self-Q-switched and wavelength-tunable tungsten disulfide-based passively Q-switched Er:Y_2O_3 ceramic lasers

Xiaofeng Guan,[1] Jiawei Wang,[1] Yuzhao Zhang,[1] Bin Xu,[1,*] Zhengqian Luo,[1] Huiying Xu,[1] Zhiping Cai,[1] Xiaodong Xu,[2,5] Jian Zhang,[3] and Jun Xu[4]

[1]Department of Electronic Engineering, Xiamen University, Xiamen 361005, China
[2]Jiangsu Key Laboratory of Advanced Laser Materials and Devices, School of Physics and Electronic Engineering, Jiangsu Normal University, Xuzhou 221116, China
[3]Key Laboratory of Transparent Opto-functional Inorganic Materials, Chinese Academy of Sciences, Shanghai 201899, China
[4]School of Physics Science and Engineering, Institute for Advanced Study, Tongji University, Shanghai 200092, China
[5]e-mail: xdxu79@mail.sic.ac.cn
*Corresponding author: xubin@xmu.edu.cn

Received 5 July 2018; accepted 8 July 2018; posted 12 July 2018 (Doc. ID 337975); published 2 August 2018

We report on diode-pumped Er:Y_2O_3 ceramic lasers at about 2.7 μm in the tunable continuous-wave, self-Q-switching and tungsten disulfide (WS_2)-based passively Q-switching regimes. For stable self-Q-switched operation, the maximum output power reaches 106.6 mW under an absorbed power of 2.71 W. The shortest pulse width is measured to be about 1.39 μs at a repetition rate of 26.7 kHz at maximum output. Using a spin-coated WS_2 as a saturable absorber, a passively Q-switched Er:Y_2O_3 ceramic laser is also realized with a maximum average output power of 233.5 mW (for the first time, to the best of our knowledge). The shortest pulse width decreases to 0.72 μs at a corresponding repetition rate of 29.4 kHz, which leads to a pulse energy of 7.92 μJ and a peak power of 11.0 W. By inserting an undoped YAG thin plate as a Fabry–Perot etalon, for the passive Q switching, wavelength tunings are also demonstrated at around 2710, 2717, 2727, and 2740 nm.

OCIS codes: (140.3480) Lasers, diode-pumped; (140.3540) Lasers, Q-switched; (140.3580) Lasers, solid-state.

https://doi.org/10.1364/PRJ.6.000830

1. INTRODUCTION

In recent years, mid-infrared lasers near 3 μm have attracted great interest because of their important applications in remote-sensing technology, atmospheric-environment monitoring, and especially in biomedical science, due to their strong water absorption and the penetration depth of a few microns in biological tissue [1,2]. Er^{3+}-doped materials make it possible to achieve 3-μm laser sources, which correspond to laser transition from $^4I_{11/2}$ to $^4I_{13/2}$ by pumping ground-state ($^4I_{15/2}$) Er^{3+} ions to the $^4I_{11/2}$ level using compact InGaAs laser diodes emitting around 970 nm [3–5]. The early research can be dated back to the 1960s, when Robinson and Devor first demonstrated a 2.69-μm stimulated emission in an erbium-doped mixed fluoride crystal [6]. After that, a variety of Er^{3+}-doped laser materials have been developed based on fluoride and oxide hosts [2–10]. In recent years, sesquioxides, as desired host materials, have excited rising research interest for high-power laser sources because of their good thermomechanical property [11–13]. Moreover, rare-earth ions doped into sesquioxides could generate ultrafast lasers because of spectral broadening of the optical transitions arising from large splitting of the ground state [14,15].

Pulsed lasers, rather than continuous-wave lasers, based on Q-switching and mode-locking technologies could have more potential in various applications. However, probably because there are no effective and easily available saturable absorbers, little early research concerning 2.8-μm Er^{3+} lasers has involved passively Q-switched and mode-locked operation. This situation is now changing with the development of 2D materials that have been reported to have advantages such as ultrabroadband saturable absorption, low cost, and easy fabrication. These merits have made 2D materials very popular for Q-switched and mode-locked laser operation from the visible to mid-infrared wavelength ranges [16–28]. In fact, in terms of passively Q-switched mid-infrared lasers as the investigated topic in this work, recently graphene [21], MoS_2 [22], tungsten disulfide (WS_2) [23], $MoTe_2$ [24], ReS_2 [25], Bi_2Te_3 [26], and black phosphorus (BP) [27,28] have been successfully used as saturable absorbers in the fields of solid-state lasers and/or fiber lasers. At present, WS_2-based mid-infrared laser operation has not yet been reported in a solid-state laser.

Transitional metal dichalcogenides (TMDs) are outstanding among 2D materials because of their superior properties of nonzero bandgap and layer-dependent third-order optical nonlinearity. Recently, as a member of TMD family, WS_2 has been developed as a saturable absorber. Similar to MoS_2, defects, boundary effects, and impurities of WS_2 could modify its bandgap structure, decreasing from 1.18 to 0.02 eV (61.6 μm) and 0.65 eV (1.89 μm) by suitably introducing W and S defects, respectively [23]. As a consequence, WS_2 should exhibit broadband saturable absorption properties, which deserves in-depth investigations.

Self-Q switching has been recognized as an interesting and effective measure for the generation of nanosecond-to-microsecond pulses with no special modulation elements to initiate and sustain the pulsing mechanism. At present, the investigation of self-Q switching has been mainly focused on near-infrared lasers. However, with respect to mid-infrared emission, it has seldom been studied. Recently, Liu *et al.* reported a self-Q-switched Er, Pr :CaF_2 laser at 2803.7 nm with a maximum output power of 262 mW; the pulse width was 718 ns [29]. A self-pulsed Er:Y_2O_3 ceramic laser has also been reported once with an average output power of 12 mW under single-end pumping geometry [30]. A more complicated laser configuration by using double-end pumping with two Er:Y_2O_3 ceramics increased the average output power to 83 mW [30]. Considering the significance of self-pulsed mid-infrared lasers and the state of the art, further investigations on this topic are still very necessary.

In this paper, stable self-Q switching has been investigated in a moderately doped Er:Y_2O_3 sesquioxide ceramic. Moreover, WS_2 has been developed for the first time as a saturable absorber for a passively Q-switched Er:Y_2O_3 laser. Additionally, by inserting an undoped YAG thin plate into the resonator, wavelength tunings of the Er:Y_2O_3 laser around 2710, 2717, 2727, and 2740 nm have also been demonstrated.

2. EXPERIMENTAL SETUP

Figure 1 shows the schematic of a diode-pumped Er:Y_2O_3 ceramic laser experimental setup. The pump source is a fiber coupled InGaAs diode laser with a core diameter of 105 μm and a numerical aperture of 0.22. The peak emitting wavelength of the diode laser is about 976 nm at a maximum output power of about 25 W at room temperature. The pump beam was focused into the Er:Y_2O_3 ceramic by two doublet lenses having focal lengths of 30 and 50 mm. Thus, the waist size of the pump beam was expanded to about 175 μm, which aimed at thermal mitigation of the laser gain medium. The flat input mirror has a transmission of about 95% at the pump wavelength and a high reflection of more than 99.9% at 2.7 μm. The 50-mm (curvature radius) output coupler has partial transmission of about 4.8% at 2.7 μm. The physical length of the laser resonator has been maintained to be about 50 mm during the experiments.

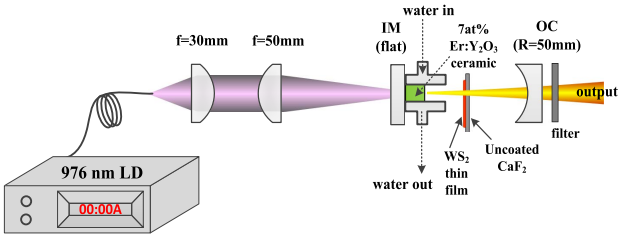

Fig. 1. Schematic of diode-pumped Er:Y_2O_3 ceramic lasers. IM, input mirror; OC, output coupler.

The laser gain medium was an Er:Y_2O_3 ceramic with a dopant concentration of 7 at. % and dimensions of $\phi 6 \times 7$ mm^3. The Er:Y_2O_3 ceramic was wrapped with a piece of indium foil and then mounted inside a water-cooled copper block with the temperature set at 13°C. The Er:Y_2O_3 absorbed about 87% of the incident pump power. An undoped YAG thin plate was used to modulate the intracavity loss for wavelength tuning. For passive Q-switching, few-layer WS_2 thin film was fabricated and transferred onto a CaF_2 substrate serving as a saturable absorber.

3. RESULTS AND DISCUSSION

In free-running mode, namely, without inserting any intracavity elements, at laser threshold the lasing behavior was observed to show a self-pulsing phenomenon only by misaligning the laser resonator. Increasing the absorbed power to about 1.46 W, stable self-Q switching was found. Figure 2 shows the dependence of average output power on absorbed power of the stable self-Q-switched Er:Y_2O_3 ceramic laser. The maximum output power reached 106.6 mW at an absorbed power of about 2.72 W. Linearly fitting the data in Fig. 2 led to a slope efficiency of about 8.2%. At the maximum output, the pulse-to-pulse amplitude fluctuation of the self-Q-switched pulse train was measured to be about ±9%. The laser spectrum measured at maximum average output power is shown as an inset in Fig. 2, which exhibits a two-peak structure with a main peak at 2717.02 nm and a side peak at 2709.9 nm. The main peak has an full width at half-maximum (FWHM) of about 2.18 nm. It should be pointed out that the dual-wavelength lasing behavior can only be observed when the average output power is close to the maximum. At threshold and low output power, only the single wavelength of 2717 nm can be found. It should be

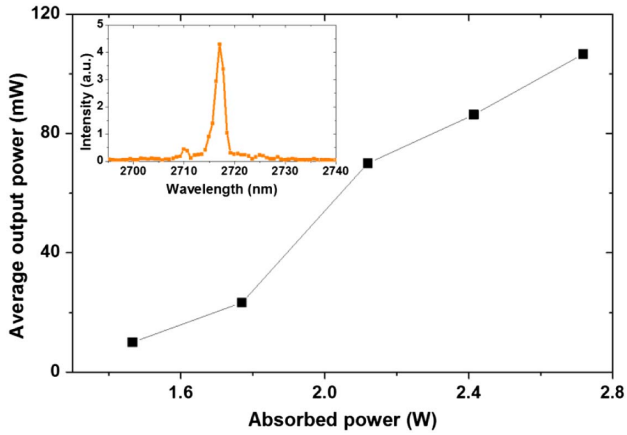

Fig. 2. Dependence of average output power on absorbed power of self-Q-switched Er:Y_2O_3 ceramic lasers; inset, corresponding laser spectrum at the highest output power.

pointed out that this result is far better than that reported in Ref. [30], with a maximum average output power of 10 mW in single-end pumping of an Er:Y_2O_3 ceramic laser. The self-pulsing phenomenon could be explained by the reabsorption effect of the Er:Y_2O_3 ceramic. As we know, lasing and spontaneous emission lead to considerable population of the $^4I_{13/2}$ lower level. The $^4I_{13/2}$ population reabsorbs the photons at the transition identical to that of laser radiation only if suitable upper and lower level lifetimes of the Er:Y_2O_3 ceramic can be satisfied [29].

Further increasing the absorbed power led to stability degradation of the self-Q-switching pulse trains. The pulse trains became disordered and finally degenerated to continuous-wave operation. This conversion from self-Q switching to continuous wave has also been observed in some other self-Q-switched lasers, e.g., Yb:CGB lasers [30,31]. To interpret this conversion phenomenon, the concentration-dependent upconversion process should be taken into account, which circumvents the well-known self-terminating effect and therefore makes it possible to lase 3-μm Er^{3+} laser radiation. However, it is also clear that increasing absorbed power will finally result in the domination of the upconversion process in contrast to the reabsorption process, which causes continuous-wave operation instead of self-pulsing, eventually. From this point of view, it seems reasonable that we have obtained higher average output power than that reported in Ref. [30]. We have used a relatively weakly doped Er:Y_2O_3 material (7% versus 15%), which is of advantage to reducing upconversion.

Figure 3 shows the typical pulse trains and the corresponding single-pulse profiles at different output powers. At the threshold, the pulse width was measured to be about 1.61 μs at a pulse repetition rate of 16.6 kHz, as shown in Fig. 3(a). At maximum output of the stable self-Q-switched laser operation, the pulse width reduced to about 1.39 μs, and the corresponding pulse repetition rate increased to 26.7 kHz, as shown in Fig. 3(b). Figure 3(c) shows a typical shape and stability-degraded pulse trains with a repetition rate of 29.1 kHz, while the pulse width was found to expand to about 1.73 μs. In fact, when the absorbed power was increased to about 3.7 W, the pulses completely collapsed, and at the same time, the output power diminished greatly. Afterward, by aligning and optimizing the laser resonator, continuous-wave laser operation can be achieved with remarkable power improvement.

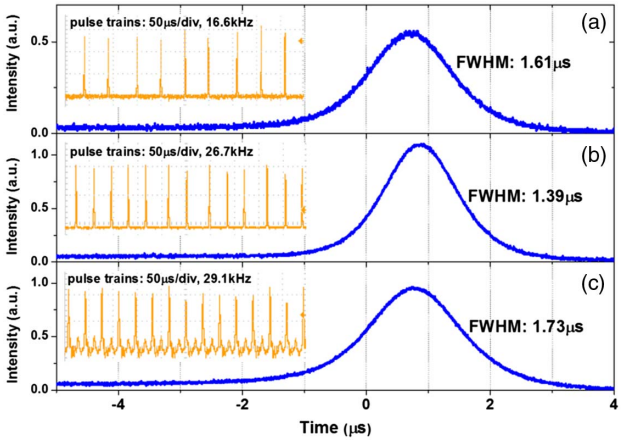

Fig. 3. Typical self-Q-switched single-pulse profiles with corresponding pulse trains as insets.

A passively Q-switched Er:Y_2O_3 ceramic laser was performed with a WS_2 saturable absorber. The few-layer WS_2 nanosheets were prepared by the liquid phase exfoliation method. The bulk WS_2 (200 mg) was sonicated for 20 h in N-2-methyl pyrrolidone (NMP, 200 mL) to produce the few-layer WS_2 suspension. The characterization of the few-layer WS_2 nanosheets is shown in Fig. 4. The bulk WS_2 and the few-layer WS_2 nanosheets are both characterized by X-ray diffraction (XRD), as shown in Fig. 4(a), in which all the labeled peaks of the bulk WS_2 correspond to hexagonal WS_2 (JCPDs NO. 08-0237). The XRD pattern of the few-layer WS_2 nanosheets only retained the c axis of the peaks, such as (002), (004), (006), and (008), and some characteristic peaks disappeared, which indicated the bulk WS_2 had been successfully exfoliated. Further, the Raman spectrum in Fig. 4(b) also confirmed the exfoliation of WS_2. The few-layer WS_2 nanosheets show E^1_{2g} and A^1_g phonon modes at 348.8 and 416.6 cm^{-1}, respectively. These values are different from bulk WS_2 (351.9 and 417.1 cm^{-1}, respectively). The mode of few-layer WS_2 redshifts compared to that of bulk WS_2, which could be attributed to the phonon softening. Besides, in Fig. 4(c), an atomic force microscopy (AFM) image was given to characterize the thickness of the as-prepared few-layer WS_2. In Fig. 4(d), the height profile indicates the as-prepared WS_2 nanosheets are around 5.52 nm, which suggests the nanosheets are about five layers, since a WS_2 monolayer is ∼1 nm [32].

The few-layer WS_2 suspension was then transferred onto a CaF_2 substrate by a simple and commonly used spin-coating method that involves dripping and rotating the WS_2 suspension onto the substrate. After drying the WS_2 suspension inside an oven with a constant temperature of 60°C for 5 h, WS_2 thin film can be formed for usage as a saturable absorber. In Fig. 5, the transmission of the blank CaF_2 substrate was measured to be about 94.5% at 2.7 μm, which corresponds to the Fresnel

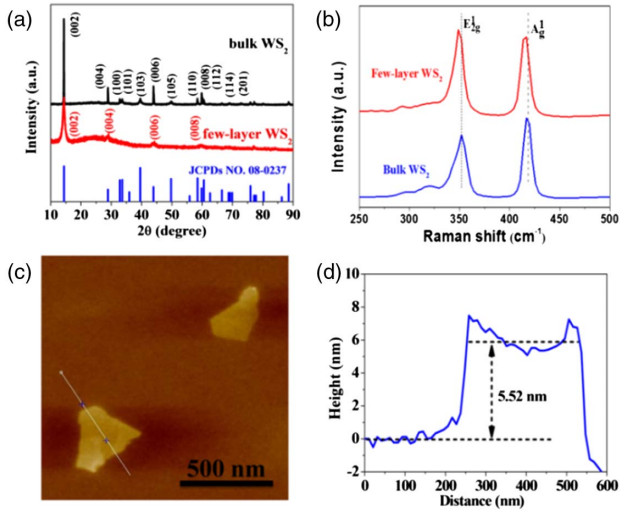

Fig. 4. (a) XRD patterns and (b) Raman spectra of the bulk WS_2 and few-layer WS_2 samples; (c) AFM image and (d) height profile of an as-prepared few-layer WS_2 sample.

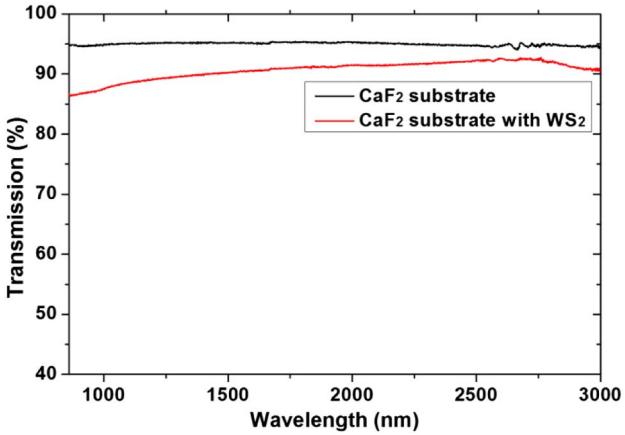

Fig. 5. Transmissions of the blank CaF_2 substrate and CaF_2 substrate with WS_2 thin film.

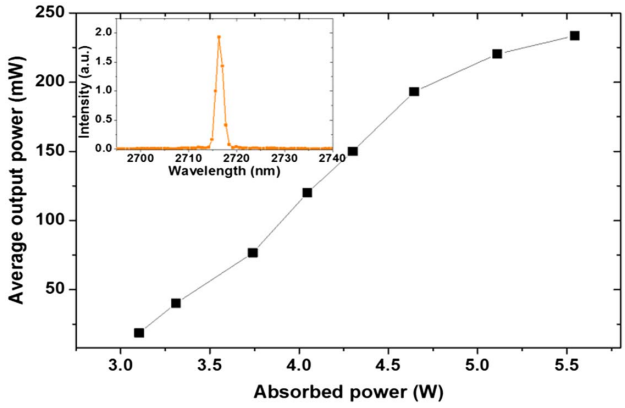

Fig. 7. Dependence of average output power on absorbed power of WS_2-based Q-switched Er:Y_2O_3 ceramic lasers; inset, corresponding laser spectrum at the highest output power.

reflection loss. The transmission indicates the transparency and good quality of the CaF_2 substrate. The as-prepared WS_2 saturable absorber, namely WS_2 thin film plus the CaF_2 substrate, was also measured to have a transmission of about 92.2% at 2.7 μm. Thus, the final transmission of the WS_2 thin film could be deduced to be around 97.5%, which means a linear loss of about 2.5%. Moreover, a broad and flat transmission in the whole near- to mid-infrared spectral range can also be found from Fig. 5, which reveals the superiority of broadband saturable absorption of the WS_2 as a saturable absorber.

The saturable absorption intensity of the WS_2 was also measured at 1960 nm with a substitute Tm^{3+}-doped mode-locked fiber laser with a pulse width of 680 fs, since a suitable 2.7-μm pulsed laser source is unavailable in our lab. In fact, according to the bandgap structure of WS_2, it should have lower saturable intensity at 2.7 μm than at 2.0 μm. Figure 6 shows the measuring result with fitted saturable intensity of 10.6 MW/cm^2, modulation depth of 6.7%, and nonsaturation loss of 6.4%.

Figure 7 shows the dependence of the average output power on the absorbed power of a WS_2-based Q-switched Er:Y_2O_3 laser with good stability. The laser threshold increased to about 3.1 W of absorbed power, which indicated a higher intracavity loss originating from the introduction of the WS_2 saturable absorber. The maximum average output power was found to be about 233.5 mW at an absorbed power of 5.54 W. Linearly fitting the data in Fig. 6 led to a slope efficiency of about 10.6%. At this maximum output, we measured the pulse-to-pulse amplitude fluctuation of the passively Q-switched pulse train to be about ±6%. We noticed that at this absorbed power, continuous-wave output power reached close to 600 mW. Optimizing the quality of the WS_2 thin film and depositing the CaF_2 substrate with antireflection coating for reducing the Fresnel loss could be resorted to for power scaling, which will be studied in our near future work. Further increasing the absorbed power led to the Q-switched pulse trains showing an instability trend. The stability degradation should arise from heat accumulation of the WS_2 thin film. The laser spectrum, showing a single-peak structure, peaks at 2716.3 nm with an FWHM of about 1.78 nm (see Fig. 7). That is to say, compared with the case of self-Q switching, the laser spectrum of passive Q switching is narrowed by 0.4 nm, which should be attributed to the etalon effect of the CaF_2 substrate.

Figure 8 shows the single-pulse profile with an FWHM value of about 0.72 μs at maximum output power. The pulse width narrowed to half the value of that of self-Q switching, which probably indicated that the modulation arising from

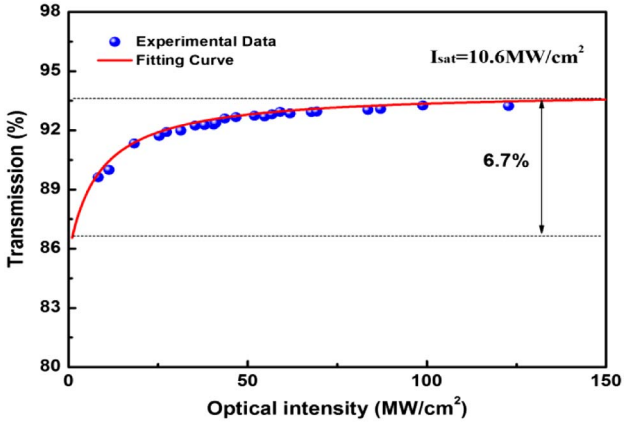

Fig. 6. Saturable absorption of the WS_2 saturable absorber used.

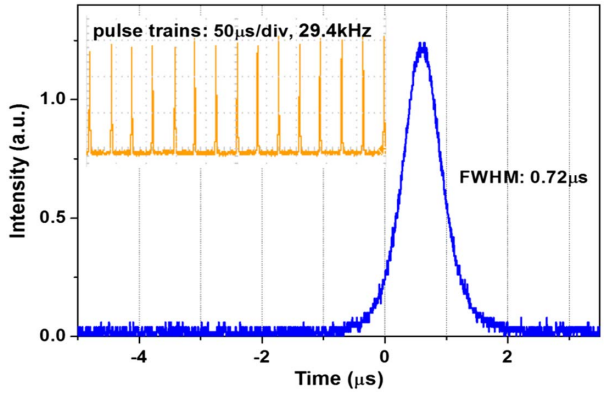

Fig. 8. Typical single-pulse profile of a passively Q-switched Er:Y_2O_3 ceramic laser; inset, corresponding pulse trains.

WS_2 is larger than that arising from reabsorption. Moreover, it is also possible that the reabsorption modulation was also introduced during the passive Q switching. In addition, one can see that the passively Q-switched laser operated at higher output than did self-Q switching with higher absorbed power, which is also helpful in producing pulses with narrower width. At maximum output, stabilities of average output power and pulse temporal profile were both measured in 1 h, as shown in Fig. 9. The stability of average output power was found to be about 4.7% with respect to the maximum average output power. For the temporal pulse profile, it has been estimated to have a time jitter of about ±0.09 μs. The recorded 0.72-μs pulse corresponded to the shortest pulse time duration.

At a large scale, the pulse trains can also be observed to have a repetition rate of 29.4 kHz. Figures 10(a) and 10(b) show the entire evolutions of pulse width and repetition rate with the increase of the absorbed powers. Basically, the pulse width shows monotonous decrease as the absorbed power increases. However, it is also very obvious that the trend of pulse narrowing is weakening. In particular, the pulse width shows saturation when reaching an absorbed power of 4.5 W. As for the pulse repetition rate, it increased from 16.7 to 29.4 kHz, showing about three-segment linear increases with decreasing slopes with the increase of the absorbed power. Knowing the pulse width and repetition rate, we further estimated the values of pulse energy and pulse peak power of the passively Q-switched Er:Y_2O_3 laser, as shown in Figs. 10(c) and 10(d). The pulse energy increased from 1.11 to 7.92 μJ, while at the same time the pulse peak power increased from 0.67 to 11.0 W.

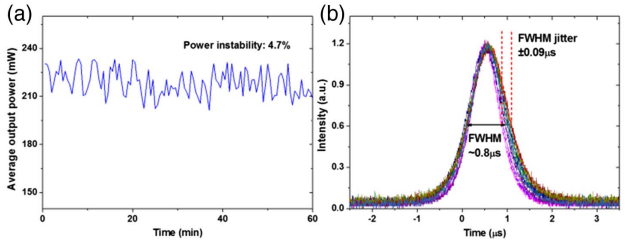

Fig. 9. (a) Stability measurement of average output power in 1 h and (b) temporal profiles of 12 superimposed pulses recorded every 5 min in 1 h.

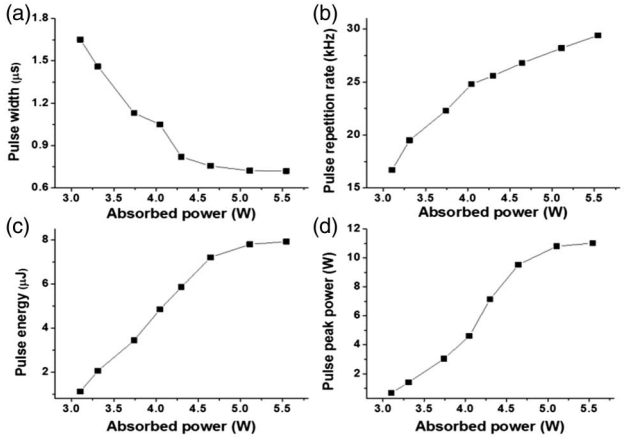

Fig. 10. Dependences of (a) pulse width, (b) pulse repetition rate, (c) pulse energy, and (d) pulse peak power on absorbed powers.

In Table 1, we compared the results of some recent research in regard to diode-pumped passively Q-switched mid-infrared solid-state lasers based on 2D material saturable absorbers. From Table 1, one can see that the present result is indeed pretty good, with relatively large output power and pulse energy. Therefore, it could be safely concluded that WS_2 as a saturable absorber applicable for mid-infrared wavelength is quite competitive with other 2D materials, and it is worth developing further.

According to the emission spectrum of Er:Y_2O_3 ceramic [33], 2717-nm emission dominates with the highest emission intensity. However, one should also notice that there are several narrow emission bands besides the 2717-nm peak, which leaves room for realizing laser operation at other emission bands. Finally, wavelength tuning was realized by adjusting the laser resonator with the help of a 0.13-mm-thick pure YAG crystal acting as a Fabry–Perot etalon with a free spectral range (FSR) of about 634 GHz. Compared with CaF_2 material, undoped YAG has a relatively larger refractive index, which is believed to produce larger transmission differences (up to about 29% instead of 7% for CaF_2) among the potential lasing wavelengths. Thus, it could allow the possibility of favoring low gain lines over high gain lines. Consequently, emission lines with lower gains could lase, which will lead to broader wavelength tuning.

The achieved laser emissions in the passively Q-switched regime are registered in Fig. 11. By slightly tilting the YAG thin plate, laser emissions around 2710, 2717, 2727, and 2740 nm have been successfully operated with a total wavelength range of about 8 nm. Some dual-wavelength laser emissions can be obtained, as shown in Fig. 11. The disconnected wavelength tuning was mainly limited by the narrow emission bands of the Er:Y_2O_3 ceramic. On the other hand, the present tuned wavelengths could indicate that mode locking is probably realizable in

Table 1. Diode-Pumped Passively Q-Switched Mid-Infrared Solid-State Lasers Based on 2D Material Saturable Absorbers

2D Material	Laser Material	Max Output Power	Min Pulse Width	Max Pulse Energy	Ref.
MoS_2	Er:Lu_2O_3	1.03 W	335 ns	8.5 μJ	[22]
$MoTe_2$	Ho, Pr:$LiLuF_4$	73 mW	670 ns	0.95 μJ	[24]
ReS_2	Er:SrF_2	0.58 W	508 ns	12.1 μJ	[25]
BP	Er:SrF_2	180 mW	702 ns	2.34 μJ	[28]
Graphene	Ho, Pr:LLF	88 mW	937.5 ns	1.6 μJ	[34]
WS_2	Er:Y_2O_3	233.5 mW	0.72 μs	7.92 μJ	This work

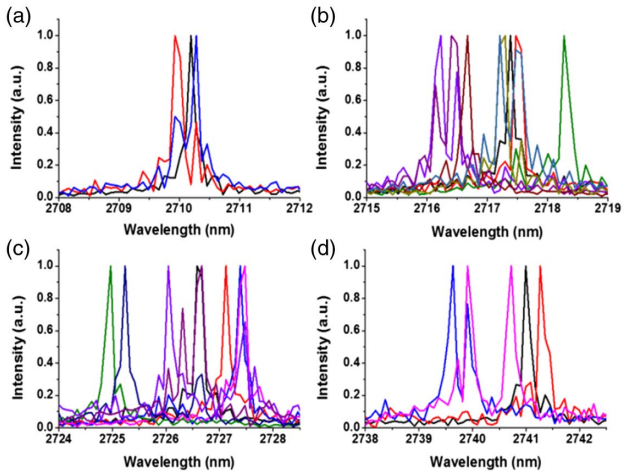

Fig. 11. Wavelength tunings of the Er:Y_2O_3 ceramic laser emissions around 2710, 2717, 2727, and 2740 nm.

Er:Y_2O_3 ceramic by configuring a laser resonator with large length.

4. CONCLUSION

In conclusion, tunable continuous-wave, self-*Q*-switched and WS_2-based passively *Q*-switched Er:Y_2O_3 ceramic lasers at about 2.7 μm have been realized. As for self-*Q*-switched operation, a maximum output power up to 106.6 mW was achieved with the shortest pulse width of about 1.39 μs at a repetition rate of 26.7 kHz. A passively *Q*-switched Er:Y_2O_3 laser has been further realized with a maximum average output power of 233.5 mW. The shortest pulse width is about 0.72 μs at a corresponding repetition rate of 29.4 kHz, which leads to a pulse energy of 7.92 μJ and a peak power of 11.0 W. Finally, wavelength tunings have also been demonstrated at around 2710, 2717, 2727, and 2740 nm by inserting an undoped YAG etalon into the laser resonator. In the near future, further power scaling of the passively *Q*-switched Er:Y_2O_3 ceramic laser could be expected by optimizing the quality of the WS_2 saturable absorber and by coating the CaF_2 substrate. Narrowing the pulse width for improving the pulse energy and peak power could also be achieved at the same time.

Funding. National Natural Science Foundation of China (NSFC) (61575164, 61575088, 11674269, 61475129); National Key Research and Development Program of China (2016YFB1102202); Natural Science Foundation of Fujian Province of China (2018J01108); Principal Fund of Xiamen University (20720180082).

REFERENCES

1. R. Kaufmann, A. Hartmann, and R. Hibst, "Cutting and skin-ablative properties of pulsed mid-infrared laser surgery," J. Dermatol. Surg. Oncol. **20**, 112–118 (1994).
2. M. Skorczakowski, J. Swiderski, W. Pichola, P. Nyga, A. Zajac, M. Maciejewska, L. Galecki, J. Kasprzak, S. Gross, A. Heinrich, and T. Bragagna, "Mid-infrared *Q*-switched Er:YAG laser for medical applications," Laser Phys. Lett. **7**, 498–504 (2010).
3. T. Jensen, A. Diening, G. Huber, and B. H. T. Chai, "Investigation of diode-pumped 2.8-μm Er:$LiYF_4$ lasers with various doping levels," Opt. Lett. **21**, 585–587 (1996).
4. C. Labbe, J. L. Doualan, P. Camy, R. Moncorge, and M. Thuau, "The 2.8 μm laser properties of Er^{3+}-doped CaF_2 crystals," Opt. Commun. **209**, 193–199 (2002).
5. D. W. Chen, C. L. Fincher, T. S. Rose, F. L. Vernon, and R. A. Fields, "Diode-pumped 1-W continuous-wave Er:YAG 3-μm laser," Opt. Lett. **24**, 385–387 (1999).
6. M. Robinson and D. P. Devor, "Thermal switching of laser emission of Er^{3+} at 2.69 μ and Tm^{3+} at 1.86 μ in mixed crystals of CaF_2:ErF_3:TmF_3," Appl. Phys. Lett. **10**, 167–170 (1967).
7. G. J. Kintz, R. Allen, and L. Esterowitz, "CW and pulsed 2.8 μm laser emission from diode-pumped Er^{3+}:$LiYF_4$ at room temperature," Appl. Phys. Lett. **50**, 1553–1555 (1987).
8. S. Wittwer, M. Pollnau, R. Spring, W. Luthy, H. P. Weber, R. A. McFarlane, C. Harder, and H. P. Meier, "Performance of a diode-pumped BaY_2F_8:Er^{3+} (7.5 at.%) laser at 2.8 μm," Opt. Commun. **132**, 107–110 (1996).
9. J. K. Chen, D. L. Sun, J. Q. Luo, H. L. Zhang, R. Q. Dou, J. Z. Xiao, Q. L. Zhang, and S. T. Yin, "Spectroscopic properties and diode end-pumped 2.79 μm laser performance of Er, Pr:GYSGG crystal," Opt. Express **21**, 23425–23432 (2013).
10. Z. Y. You, Y. Wang, J. L. Xu, Z. J. Zhu, J. F. Li, H. Y. Wang, and C. Y. Tu, "Single-longitudinal-mode Er:GGG microchip laser operating at 2.7 μm," Opt. Lett. **40**, 3846–3848 (2015).
11. P. A. Loiko, K. V. Yumashev, R. Schödel, M. Peltz, C. Liebald, X. Mateos, B. Deppe, and C. Kränkel, "Thermo-optic properties of Yb:Lu_2O_3 single crystals," Appl. Phys. B **120**, 601–607 (2015).
12. Z. Y. Zhou, X. Guan, X. Huang, B. Xu, H. Xu, Z. Cai, X. Xu, P. Liu, D. Li, J. Zhang, and J. Xu, "Tm^{3+}-doped $LuYO_3$ mixed sesquioxide ceramic laser: effective 2.05-μm source operating in continuous-wave and passive *Q*-switching regimes," Opt. Lett. **42**, 3781–3784 (2017).
13. L. Wang, H. T. Huang, D. Y. Shen, J. Zhang, H. Chen, Y. Wang, X. Liu, and D. Y. Tang, "Room temperature continuous-wave laser performance of LD pumped Er:Lu_2O_3 and Er:Y_2O_3 ceramic at 2.7 μm," Opt. Express **22**, 19495–19503 (2014).
14. G. Q. Xie, D. Y. Tang, L. M. Zhao, L. J. Qian, and K. Ueda, "High-power self-mode-locked Yb:Y_2O_3 ceramic laser," Opt. Lett. **32**, 2741–2743 (2007).
15. A. Schmidt, P. Koopmann, G. Huber, P. Fuhrberg, S. Y. Choi, D. Yeom, F. Rotermund, V. Petrov, and U. Griebner, "175 fs Tm:Lu_2O_3 laser at 2.07 μm mode-locked using single-walled carbon nanotubes," Opt. Express **20**, 5313–5318 (2012).
16. Y. Zhang, H. Yu, R. Zhang, G. Zhao, H. Zhang, Y. Chen, L. Mei, M. Tonelli, and J. Wang, "Broadband atomic-layer MoS_2 optical modulators for ultrafast pulse generations in the visible range," Opt. Lett. **42**, 547–550 (2017).
17. Y. Jhon, J. Koo, B. Aansori, M. Seo, J. H. Lee, Y. Gogotsi, and Y. M. Jhon, "Metallic MXene saturable absorber for femtosecond mode-locked lasers," Adv. Mater. **29**, 1702496 (2017).
18. B. Xu, Y. Cheng, Y. Wang, Y. Huang, J. Peng, Z. Luo, H. Xu, Z. Cai, J. Weng, and R. Moncorgé, "Passively *Q*-switched Nd:$YAlO_3$ nanosecond laser using MoS_2 as saturable absorber," Opt. Express **22**, 28934–28940 (2014).
19. L. C. Kong, G. Q. Xie, P. Yuan, L. J. Qian, S. X. Wang, H. H. Yu, and H. J. Zhang, "Passive *Q*-switching and *Q*-switched mode-locking operations of 2 μm Tm:CLNGG laser with MoS_2 saturable absorber mirror," Photon. Res. **3**, A47–A50 (2015).
20. B. Xu, Y. Wang, J. Peng, Z. Luo, H. Xu, Z. Cai, and J. Weng, "Topological insulator Bi_2Se_3 based *Q*-switched Nd:$LiYF_4$ nanosecond laser at 1313 nm," Opt. Express **23**, 7674–7680 (2015).
21. X. Guan, L. Zhan, Z. Zhu, B. Xu, H. Xu, Z. Cai, W. Cai, X. Xu, J. Zhang, and J. Xu, "Continuous-wave and CVD-graphene-based passively *Q*-switched Er:Y_2O_3 ceramic lasers at 2.7 μm," Appl. Opt. **57**, 371–376 (2018).
22. M. Fan, T. Li, S. Zhao, G. Li, H. Ma, X. Gao, C. Krankel, and G. Huber, "Watt-level passively *Q*-switched Er:Lu_2O_3 laser at 2.84 μm using MoS_2," Opt. Lett. **41**, 540–543 (2016).
23. C. Wei, H. Y. Luo, H. Zhang, C. Li, J. T. Xie, J. F. Li, and Y. Liu, "Passively *Q*-switched mid-infrared fluoride fiber laser around 3 μm

using a tungsten disulfide (WS_2) saturable absorber," Laser Phys. Lett. **13**, 105108 (2016).
24. Z. Yan, T. Li, S. Zhao, K. Yang, D. Li, G. Li, S. Zhang, and Z. Gao, "$MoTe_2$ saturable absorber for passively *Q*-switched Ho, Pr:$LiLuF_4$ laser at 3 μm," Opt. Laser Technol. **100**, 261–264 (2018).
25. M. Fan, T. Li, J. Zhao, S. Zhao, G. Li, K. Yang, L. Su, H. Ma, and C. Krankel, "Continuous wave and ReS_2 passively *Q*-switched Er:SrF_2 laser at ∼3 μm," Opt. Lett. **43**, 1726–1729 (2018).
26. J. F. Li, H. Y. Luo, L. L. Wang, C. J. Zhao, H. Zhang, H. P. Li, and Y. Liu, "3-μm mid-infrared pulse generation using topological insulator as the saturable absorber," Opt. Lett. **40**, 3659–3662 (2015).
27. Z. P. Qin, G. Q. Xie, H. Zhang, C. J. Zhao, P. Yuan, S. C. Wen, and L. J. Qian, "Black phosphorus as saturable absorber for the *Q*-switched Er:ZBLAN fiber laser at 2.8 μm," Opt. Express **23**, 24713–24718 (2015).
28. J. Liu, J. Liu, Z. Guo, H. Zhang, W. Ma, J. Wang, and L. Su, "Dual-wavelength *Q*-switched Er:SrF_2 laser with a black phosphorus absorber in the mid-infrared region," Opt. Express **24**, 30289–30295 (2016).
29. J. J. Liu, X. W. Fan, J. Liu, W. W. Ma, J. Y. Wang, and L. B. Su, "Mid-infrared self-*Q*-switched Er, Pr:CaF_2 diode-pumped laser," Opt. Lett. **41**, 4660–4663 (2016).
30. H. T. Huang, L. Wang, D. Y. Shen, J. Zhang, and D. Y. Tang, "Self-pulsed nanosecond 2.7-μm solid-state erbium laser by cooperatively enhanced reabsorption," IEEE Photon. J. **7**, 1504207 (2015).
31. J. L. Xu, Y. Ji, Y. Wang, Z. You, H. Wang, and C. Y. Tu, "Self-*Q*-switched, orthogonally polarized, dual-wavelength laser using long-lifetime Yb^{3+} crystal as both gain medium and saturable absorber," Opt. Express **22**, 6577–6582 (2014).
32. H. R. Gutiérrez, N. P. López, A. L. Elías, A. Berkdemir, B. Wang, R. Lv, F. Urías, V. H. Crespi, H. Terrones, and M. Terrones, "Extraordinary room-temperature photoluminescence in triangular WS_2 monolayers," Nano Lett. **13**, 3447–3454 (2013).
33. T. Sanamyan, J. Simmons, and M. Dubinskii, "Er^{3+}-doped Y_2O_3 ceramic laser at ∼2.7 μm with direct diode pumping of the upper laser level," Laser Phys. Lett. **7**, 206–209 (2010).
34. H. Nie, P. Zhang, B. Zhang, K. Yang, L. Zhang, T. Li, S. Zhang, J. Xu, Y. Hang, and J. He, "Diode-end-pumped Ho, Pr:$LiLuF_4$ bulk laser at 2.95 μm," Opt. Lett. **42**, 699–702 (2017).